https://doi.org/10.48047/AFJBS.6.14.2024.10131-10143

African Journal of Biological Sciences

Journal homepage: http://www.afjbs.com

Research Paper Open Access

"Design and Synthesis of 4,5,6,7-Tetrahydrobenzo[b]thiophene Derivatives: A Computational Approach to EGFR Inhibition and Anticancer Activity"

Parag G Ingole.[1]*, Vivek B Panchabhai.[1], Santosh R. Butle [1]

[1]*School of Pharmacy, Swami Ramanand Teerth Marathwada University, Nanded-431606, Maharashtra, India*

***Corresponding author:** Parag G. Ingole, School of Pharmacy, Swami Ramanand Teerth Marathwada University, Nanded-431606, Maharashtra, India

Email: ingoleparag@gmail.com

Volume 6, Issue 14, Aug 2024

Received: 15 June 2024

Accepted: 25 July 2024

Published: 29 Aug 2024

doi: 10.48047/AFJBS.6.14.2024.10131-10143

ABSTRACT:

This study explores the development of 4,5,6,7-tetrahydrobenzo[b]thiophene derivatives as potential EGFR inhibitors with anticancer activity. Molecular docking identified three key compounds—PI 13, PI 40, and PI 5—with strong binding affinities, influenced by electron-withdrawing groups like hydroxyl groups on the aromatic ring. These compounds were synthesized and tested for anticancer efficacy using the MTT assay on MCF-7 cells. PI 13 showed the highest potency (IC50 = 0.062 μM), with PI 40 and PI 5 also demonstrating significant activity. The results confirm a strong correlation between docking predictions and biological activity, supporting their potential as targeted anticancer agents.

Keywords: 4,5,6,7-tetrahydrobenzo[b]thiophene, EGFR inhibitors, MTT assay, anticancer, Docking

INTRODUCTION:

Epidermal growth factor receptor (EGFR), a member of the receptor tyrosine kinase (RTK) family, is also known as phosphotyrosine kinase. RTKs are single-pass transmembrane proteins essential for intercellular signaling, translating extracellular signals (such as ligands or growth factors) into specific intracellular signaling pathways that regulate cell division and

differentiation. The RTK family includes four key members: EGFR (HER-1/ErbB-1), HER-2 (ErbB-2), HER-3 (ErbB-3), and HER-4 (ErbB-4).[1-3]

Tyrosine kinase receptors are activated upon ligand binding (e.g., EGF, TGFA), leading to receptor dimerization—either homodimers (EGFR-EGFR) or heterodimers (e.g., EGFR-HER2, EGFR-HER3, EGFR-HER4)[4]. This dimerization activates the tyrosine kinase domain, resulting in autophosphorylation on multiple tyrosine residues. This activation triggers a cascade of intracellular signaling pathways that influence gene transcription, ultimately promoting cancer cell proliferation, inhibiting apoptosis, enhancing invasion and metastasis, and stimulating tumor-induced angiogenesis.[5]

EGFR is frequently aberrantly expressed or mutated in various cancers, playing a pivotal role in tumor progression. Its involvement in solid tumors, such as those of the head and neck, lung, breast, bladder, prostate, and kidney, makes it a prime target for anticancer therapies.[6-7] EGFR and HER-2 are central targets in cancer research, with inhibitors like Gefitinib and Erlotinib, approved by the US FDA, used to treat non-small-cell lung cancer (NSCLC).[8]

EXPERIMENTAL:

Materials and Methods: Chemicals sourced from S. D. Fine Chemicals (Mumbai) were of LR grade, and GR grade solvents were utilized. The progress of reactions and the purity of compounds were assessed using Merck TLC plates, along with UV light and iodine fumes for detection. Products were purified through standard workup procedures followed by recrystallization, and their purity was confirmed via single-spot analysis on TLC. IR spectra were recorded using a Shimadzu FTIR-8400s spectrophotometer, and melting points were determined with a VEEGO VMP-D apparatus (uncorrected). Proton NMR (1H NMR) spectra were acquired on a Varian-NMR-Mercury 300 using $CDCl_3$ as the solvent, and LC–ESI/MS provided accurate mass measurements to four decimal places.

Molecular Docking Studies:

1. **Receptor Selection:** Docking simulations were performed using the epidermal growth factor receptor (PDB ID: 1M17) in complex with the selective inhibitor AQ-4 ([6,7-bis(2-methoxy-ethoxy)quinazoline-4-yl]-(3-ethynylbenzyl)amine). The receptor structure, resolved by X-ray diffraction, was obtained from the Protein Data Bank.[11]
2. **Ligand Drawing:** Potential ligands were constructed using the build panel in the Maestro graphical user interface. The ligands were designed to exhibit a range of substituents on a common scaffold, as depicted in Figure 1. A comprehensive list of these ligands is provided in Table 1.
3. **Ligand Preparation:** Ligand preparation was performed using the LigPrep panel in Maestro. This process generated a single low-energy 3D structure with accurate chirality for each ligand. Structures in .mae format were imported and prepared using the OPLS 2005 force field. Ionization states were adjusted for pH 7.0 ± 2.0, and only one low-energy ring conformer and stereoisomer per ligand were considered.

4. **Protein and Ligand Complex Preparation:** To ensure high-quality docking results, the protein structures were prepared by adding hydrogens and correcting charge states and steric clashes. Initial protein structures from the Protein Data Bank often lacked hydrogens and had unusual residue charges, so these were adjusted, and water molecules were removed. Ligand, cofactor, and nonstandard residue bond orders and charges were also corrected. Protein preparation included neutralizing residues within 10–20 Å of the ligand and performing restrained minimizations to optimize hydrogen positions and resolve structural strain. The optimized enzyme structure (1M17) and ligand AQ-4 are shown in Figure 2, respectively.

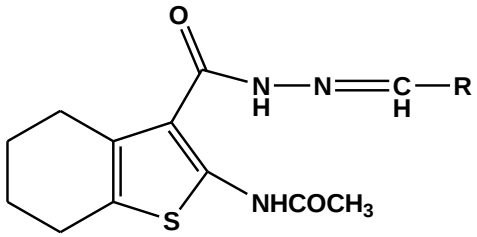

Figure 1: PI series of derivatives containing 54 compounds

Table 1: PI series containing 54 compounds

S.N.	Compound code	R	S.N.	Compound code	R
1	PI 1	Benzyl	28	PI 28	3 -F, 4 -Br Benzyl
2	PI 2	4-Cl Benzyl	29	PI 29	2 -F, 5 -Br Benzyl
3	PI 3	3-NO_2 Benzyl	30	PI 30	4-bromofuran-2-yl
4	PI 4	2,3,4 tri OH Benzyl	31	PI 31	5-bromofuran-2-yl
5	PI 5	2, 4 di-OH Benzyl	32	PI 32	5-nitrofuran-2-yl
6	PI 6	3-OH Benzyl	33	PI 33	3 -Br, 4 – OCH_3Benzyl
7	PI 7	2-F Benzyl	34	PI 34	2 – OCH_3, 4 -Br Benzyl
8	PI 8	3,4-di OH Benzyl	35	PI 35	2 – OCH_3, 5 -Br Benzyl
9	PI 9	3,4 di F Benzyl	36	PI 36	2 -OH, 3 – Br, 5 -NO_2 Benzyl
10	PI 10	2 -CH_3 Benzyl	37	PI 37	2 -OH, 3 – NO_2, 5 -Br Benzyl
11	PI 11	3 -CH_3 Benzyl	38	PI 38	2 -OH, 3 – CF_3 Benzyl
12	PI 12	2,4 di -CH_3 Benzyl	39	PI 39	2-bromopyridin-4-yl
13	PI 13	2,4,5 tri OH Benzyl	40	PI 40	5-bromopyridin-2-yl
14	PI 14	2, 4 -di CF_3 Benzyl	41	PI 41	5-bromopyridin-3-yl
15	PI 15	2, 5 -di CF_3 Benzyl	42	PI 42	6-bromopyridin-2-yl
16	PI 16	3, 5 -di CF_3 Benzyl	43	PI 43	2,3,4 -tri OCH_3 Benzyl
17	PI 17	2 -Br Benzyl	44	PI 44	3,4,6 -tri OCH_3 Benzyl
18	PI 18	3 -Br Benzyl	45	PI 45	2,4,6 -tri OCH_3 Benzyl
19	PI 19	4 -Br Benzyl	46	PI 46	3,4,5 -tri OCH_3 Benzyl
20	PI 20	2 -Cl, 4 – Br Benzyl	47	PI 47	4 -SCF_3 Benzyl

21	PI 21	2 -Br, 3 -F, 6- F Benzyl	48	PI 48	2 – NO_2 Benzyl
22	PI 22	2 -F, 3 -Br, 6- F Benzyl	49	PI 49	4 – NO_2
23	PI 23	3 -F, 4 -Br, 6- F Benzyl	50	PI 50	2- Cl, 3 -F
24	PI 24	2 -F, 3 -F, 6- Br Benzyl	51	PI 51	2- Cl, 4 -F
25	PI 25	3 -F, 6- Br Benzyl	52	PI 52	2- Cl, 6 -F
26	PI 26	3 -Br, 4 -F Benzyl	53	PI 53	2 -F, 3- Cl
27	PI 27	2 -F, 4 -Br Benzyl	54	PI 54	3- Cl, 4-F

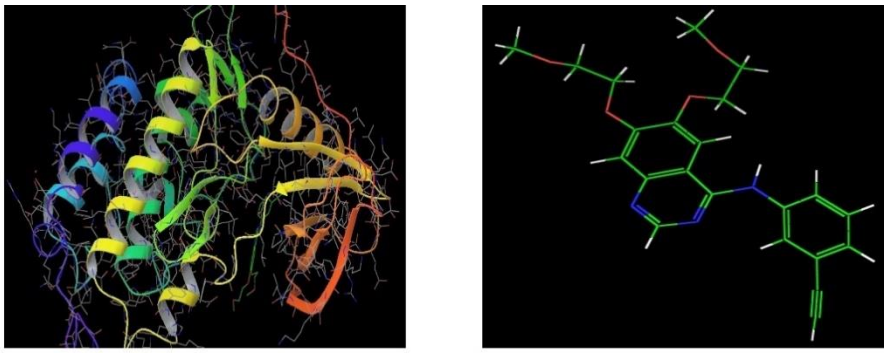

Figure 2: 1M17 enzyme structure and Co-crystallized Ligand AQ4

5. **Receptor Grid Generation:** A grid file was generated to define the receptor's active site for ligand docking. The grid encompassed the volume of the protein as indicated by the purple box in Figure 3. The grid was centered on the centroid of the workspace ligand, with default size settings to accommodate ligands similar in size. No additional constraints were applied during grid preparation.

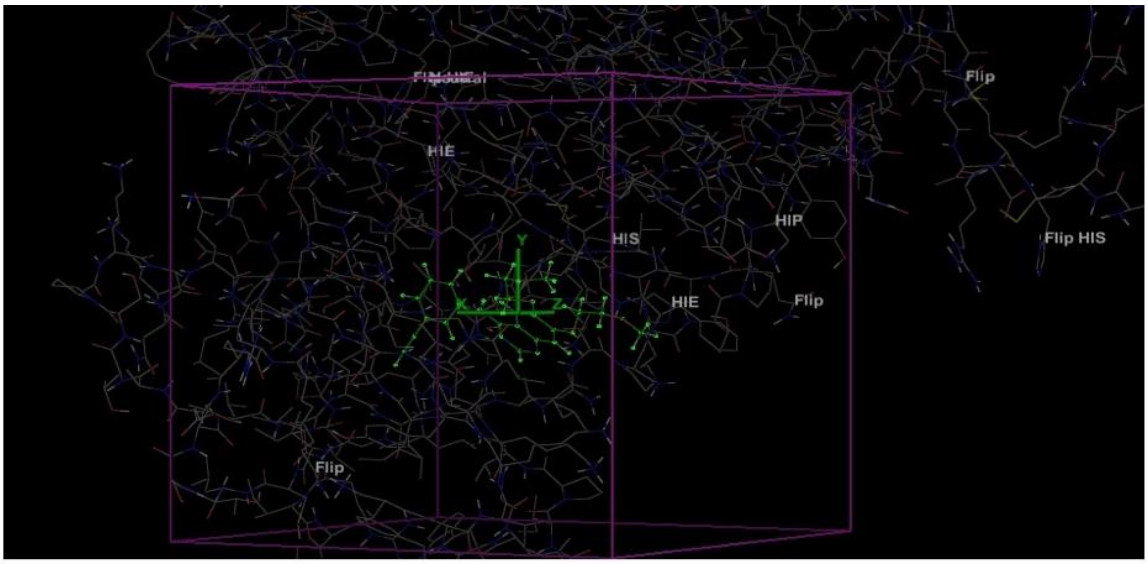

Figure 3: The Marked Ligand AQ4 with enclosing box (Pink Colour)

6. Ligand Docking: Docking was performed using the Extra Precision (XP) mode, allowing flexibility for 5- and 6-membered ring flips. Two sets of ligands were docked and scored without

similarity scoring. Ligands with more than 120 atoms or 20 rotatable bonds were excluded. Each ligand was docked to yield one pose, which was recorded in the pose viewer file. Van der Waals radius scaling for ligand atoms was set to default, with scaling factors of 0.80 for atoms with partial atomic charges below 0.15.

Synthesis of N-(3-(2-substituted hydrazinecarbonyl)-4,5,6,7-tetrahydrobenzo[b]thiophen-2-yl)acetamide derivatives [12-14]

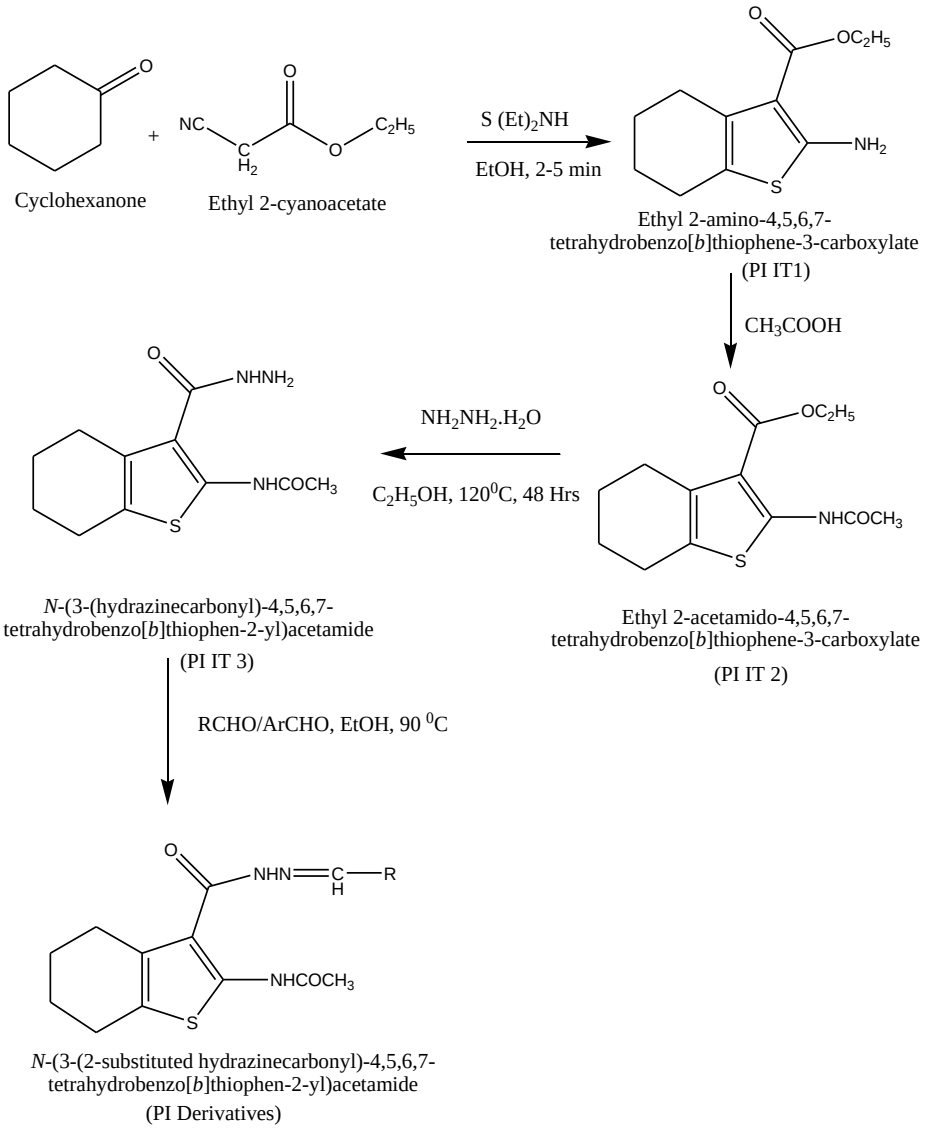

Synthetic scheme for PI Series compounds

Step 1: Synthesis of Ethyl 2-amino-4,5,6,7-tetrahydrobenzo[b]thiophene-3-carboxylate (PIIT 1): Mix cyclohexanone (0.05 mol), sulfur (1.6 g, 0.05 mol), ethyl cyanoacetate (5.8 g, 0.05 mol), and diethylamine (3.65 g, 0.05 mol) in ethanol (4 mL) in a 100-mL glass beaker. Irradiate with microwave at 350 W for 2-5 minutes. After cooling, filter the product, wash with chilled aqueous ethanol, and dry. *Yield:* 94.24%. *Melting Point:* 116-118°C. *IR (KBr) cm⁻¹:* 3371, 3297, 2977, 1718, 1458. *¹H NMR (DMSO-d6, 400 MHz) δ:* 1.40 (t, 3H, CH_3), 1.67-1.69 (m, 1H, CH_2 {Ring}), 2.61-2.63 (m, 1H, CH_2 {Ring}), 4.35 (q, 1H, -CH_2), 7.67 (s, 2H, NH_2). *HRMS (EI) m/z:* Calcd for $C_{11}H_{15}NO_2S$ 225.31, found 225.31.

Step 2: Synthesis of Ethyl 2-acetamido-4,5,6,7-tetrahydrobenzo[b]thiophene-3-carboxylate (PIIT 2): React ethyl 2-amino-4,5,6,7-tetrahydrobenzo[b]thiophene-3-carboxylate (0.05 mol) with excess acetic acid for 5 hours. Neutralize with ammonia solution and filter the product. *Yield:* 86.89%. *Melting Point:* 142-145°C. *IR (KBr) cm⁻¹:* 3383, 2943, 1720, 1652, 1447. *¹H NMR (DMSO-d6, 400 MHz) δ:* 1.39 (t, 3H, CH_3), 1.67-1.69 (m, 1H, CH_2 {Ring}), 2.61-2.83 (m,

1H, CH_2 {Ring}), 4.36 (q, 1H, -CH_2), 4.95 (s, 1H, NH). *HRMS (EI) m/z:* Calcd for $C_{13}H_{17}NO_3S$ 267.34, found 267.34.

Step 3: Synthesis of N-(3-(hydrazinecarbonyl)-4,5,6,7-tetrahydrobenzo[b]thiophen-2-yl)acetamide (PIIT 3): Add hydrazine hydrate (15 mol) to ethyl 2-acetamido-4,5,6,7-tetrahydrobenzo[b]thiophene-3-carboxylate (12 mol). Include ethanol (3 mL, 12 mol) and heat the mixture in a round-bottom flask at 90°C for 48 hours. Filter and recrystallize the product. *Yield:* 89.46%. *Melting Point:* 138-140°C. *IR (KBr) cm^{-1}:* 3367, 3298, 2977, 1695, 1652, 1451. *^{1}H NMR (DMSO-d6, 400 MHz) δ:* 1.67-1.69 (m, 1H, CH_2 {Ring}), 1.87 (s, 2H, NH_2), 2.61-2.83 (m, 1H, CH_2 {Ring}), 4.42 (s, 1H, -NH), 8.42 (s, 1H, NH). *HRMS (EI) m/z:* Calcd for $C_{11}H_{15}N_3O_2S$ 253.32, found 253.32.

Step 4: General Procedure for N-(3-(2-substituted hydrazinecarbonyl)-4,5,6,7-tetrahydrobenzo[b]thiophen-2-yl)acetamide (PI Derivatives): Heat a mixture of N-(3-(hydrazinecarbonyl)-4,5,6,7-tetrahydrobenzo[b]thiophen-2-yl)acetamide (1 mmol) and a substituted aliphatic/aromatic aldehyde (1 mmol) in ethanol (5 mL) under reflux with stirring for 30 minutes. Add water (5 mL), filter the precipitated product, and recrystallize from ethanol.

4.1:- *N*-(3-{[(2*E*)-2-benzylidenehydrazinyl]carbonyl}-4,5,6,7-tetrahydro-1-benzothiophen-2-yl)acetamide (PI 1): Yield: 92.12%. mp: 165-167°C. IR (KBr) cm^{-1}: 3371, 3297, 2977, 1718, 1458. ^{1}H NMR (DMSO-d6, 400 MHz) δ: 1.70-1.71 (m, 1H, -CH2), 2.22 (s, 2H, CH_3), 2.61-2.83 (m, 1H, CH2 {Ring}), 6.91 (s, 1H, -CONH), 7.32-7.35 (m, 2H, Ar), 8.88 (s, 1H, N=CH). HRMS (EI) m/z calcd for $C_{18}H_{19}N_3O_2S$ 341.43, found 341.43.

4.2:- *N*-(3-{[(2*E*)-2-(2,4-dihydroxybenzylidene)hydrazinyl]carbonyl}-4,5,6,7-tetrahydro-1-benzothiophen-2-yl)acetamide (PI 5): Yield: 95.46%. mp: 157-159°C. IR (KBr) cm^{-1}: 3383, 2943, 1720, 1657, 1447. ^{1}H NMR (DMSO-d6, 400 MHz) δ: 1.69-1.71 (m, 1H, CH2 {Ring}), 2.22 (s, 2H, CH_3), 2.61-2.83 (m, 1H, CH2 {Ring}), 4.02 (s, 1H, -OH), 6.56 (s, 1H, -Ar), 7.13-7.61 (m, 2H, Ar), 8.92 (s, 1H, N=CH). HRMS (EI) m/z calcd for $C_{18}H_{19}N_3O_4S$ 373.43, found 373.32.

4.3:-*N*-(3-{[(2*E*)-2-(3-hydroxybenzylidene)hydrazinyl]carbonyl}-4,5,6,7-tetrahydro-1-benzothiophen-2-yl)acetamide (PI 6): Yield: 85.65%. mp: 159-161°C. IR (KBr) cm^{-1}: 3325, 3228, 2979, 1658, 1548. ^{1}H NMR (DMSO-d6, 400 MHz) δ: 1.70-1.71 (m, 1H, CH2 {Ring}), 2.26 (s, 1H, CH3), 2.61-2.83 (m, 1H, CH2 {Ring}), 3.81 (s, 1H, -OH), 6.56 -7.33 (m, 2H, Ar), 7.40(s, 1H, CONH). 7.80 (s, 1H, N=CH). HRMS (EI) m/z calcd for $C_{18}H_{19}N_3O_3S$ 357.43, found 357.43.

4.4:- *N*-(3-{[(2*E*)-2-(3,4-dihydroxybenzylidene)hydrazinyl]carbonyl}-4,5,6,7-tetrahydro-1-benzothiophen-2-yl)acetamide (PI 8): Yield: 85.25%. mp: 166-167°C. IR (KBr) cm^{-1}: 3370, 3224, 3150, 2976, 1664, 1456. ^{1}H NMR (DMSO-d6, 400 MHz) δ: 1.70-1.71 (m, 1H, CH2 {Ring}), 2.22 (s, 1H, CH3), 2.61-2.83 (m, 1H, CH2 {Ring}), 3.52 (s, 1H, -OH), 6.35 -7.18 (m, 2H, Ar), 7.71(s, 1H, CONH). 8.84 (s, 1H, N=CH). HRMS (EI) m/z calcd for $C_{18}H_{19}N_3O_4S$ 373.43, found 373.43.

4.5:-*N*-(3-{[(2*E*)-2-(2-methoxybenzylidene)hydrazinyl]carbonyl}-4,5,6,7-tetrahydro-1-benzothiophen-2-yl)acetamide (PI 10): Yield: 96.89%. mp: 164-167°C. IR (KBr) cm^{-1}: 3377, 3020,

2918, 1690. ^{1}H NMR (DMSO-d6, 400 MHz) δ: 1.67-1.68 (m, 1H, CH2 {Ring}), 2.26 (s, 1H, CH3), 2.33 (s, 1H, -CH3 Ar), 2.61-2.83 (m, 1H, CH2 {Ring}), 6.53 (s, 1H, -CONH), 7.12 -7.52 (m, 2H, Ar), 9.37 (s, 1H, N=CH). HRMS (EI) m/z calcd for $C_{19}H_{21}N_3O_2S$ 355.45, found 355.45.

4.6:- *N*-(3-{[(2*E*)-2-(2,4,5-trihydroxybenzylidene)hydrazinyl]carbonyl}-4,5,6,7-tetrahydro-1-benzothiophen-2-yl)acetamide (PI 13): Yield: 92.47%. mp: 145-147°C. IR (KBr) cm^{-1}: 3386, 3276, 3067, 2919, 1688, 1472. ^{1}H NMR (DMSO-d6, 400 MHz) δ: 1.70-1.71 (m, 1H, CH2 {Ring}), 2.26 (s, 2H, CH_3), 2.61-2.83 (m, 1H, CH2 {Ring}), 3.48 (s, 1H, -OH), 8.47 (s, 1H, -CONH), 6.50-6.67 (m, 2H, Ar), 9.12 (s, 1H, N=CH). HRMS (EI) m/z calcd for $C_{18}H_{19}N_3O_5S$ 389.43, found 389.43.

4.7:- *N*-(3-{[(2*E*)-2-(4-bromo-3-fluorobenzylidene)hydrazinyl]carbonyl}-4,5,6,7-tetrahydro-1-benzothiophen-2-yl)acetamide (PI 28): Yield: 79.85%. mp: 154-157°C. IR (KBr) cm^{-1}: 3386, 3276, 3067, 2919, 1688. ^{1}H NMR (DMSO-d6, 400 MHz) δ: 1.70-1.71 (m, 1H, CH2 {Ring}), 2.22 (s, 2H, CH_3), 2.61-2.83 (m, 1H, CH2 {Ring}), 6.89 (s, 1H, -CONH), 6.53-7.67 (m, 2H, Ar), 8.86 (s, 1H, N=CH).HRMS (EI) m/z calcd for $C_{18}H_{17}BrFN_3O_2S$ 438.31, found 438.31.

4.8:- *N*-[3-(1-{(2*E*)-2-[(4-bromofuran-2-yl)methylidene]hydrazinyl}ethyl)-4,5,6,7-tetrahydro - 1-benzothiophen-2-yl]acetamide (PI 30): Yield: 88.31%. mp: 165-167°C. IR (KBr) cm^{-1}: 3369, 3027, 2918, 1687. 678. ^{1}H NMR (DMSO-d6, 400 MHz) δ: 1.67-1.68 (m, 1H, CH2 {Ring}), 2.25 (s, 2H, CH_3), 2.61-2.83 (m, 1H, CH2 {Ring}), 5.90 (s, 1H, -Furan), 8.47 (s, 1H, -CONH), 6.50-6.67 (m, 2H, Ar), 8.79 (s, 1H, N=CH).HRMS (EI) m/z calcd for $C_{16}H_{16}BrN_3O_3S$ 410.29, found 410.29.

4.9:- *N*-[3-(1-{(2*E*)-2-[(5-bromofuran-2-yl)methylidene]hydrazinyl}ethyl)-4,5,6,7-tetrahydro -1-benzothiophen-2-yl]acetamide (PI 31): Yield: 86.65%. mp: 159-161°C. IR (KBr) cm^{-1}: 3373, 3027, 2920, 1660, 687. ^{1}H NMR (DMSO-d6, 400 MHz) δ: 1.74-1.75 (m, 1H, CH2 {Ring}), 2.25 (s, 2H, CH_3), 2.62-2.82 (m, 1H, CH2 {Ring}), 3.48 (s, 1H, -OH), 8.47 (s, 1H, -CONH), 6.50-6.67 (m, 2H, Ar), 9.49 (s, 1H, N=CH). HRMS (EI) m/z calcd for $C_{16}H_{16}BrN_3O_3S$ 410.29, found 410.29.

4.10:- *N*-(3-{[(2*E*)-2-(3-bromo-2-fluro-5-nitrobenzylidene)hydrazinyl]carbonyl}-4,5,6,7tetra hydro-1-benzothiophen-2-yl)acetamide (PI 36): Yield: 86.58%. mp: 157-159°C. IR (KBr) cm^{-1}: 3382, 3371, 3087, 2921, 1676, 1352, 685 . ^{1}H NMR (DMSO-d6, 400 MHz) δ: 1.68-1.69 (m, 1H, CH2 {Ring}), 2.29 (s, 2H, CH_3), 2.61-2.83 (m, 1H, CH2 {Ring}), 6.24 (s, 1H, -CONH), 8.08-8.44 (m, 2H, Ar), 9.70 (s, 1H, N=CH) 10.19 (s, 1H, -OH). HRMS (EI) m/z calcd for $C_{18}H_{17}BrN_4O_5S$ 481.32, found 481.32.

4.11:- *N*-[3-(1-{(2*Z*)-2-[(2-bromopyridin-4-yl)methylidene]hydrazinyl}ethyl)-4,5,6,7-tetra hydro-1-benzothiophen-2-yl]acetamide (PI 39): Yield: 85.92%. mp: 164-167°C. IR (KBr) cm^{-1}: 3293, 3074, 2979, 1659, 690. ^{1}H NMR (DMSO-d6, 400 MHz) δ: 1.70-1.71 (m, 1H, CH2 {Ring}), 2.26 (s, 2H, CH_3), 2.61-2.83 (m, 1H, CH2 {Ring}), 7.42 (s, 1H, -CONH), 7.93-8.61 (m, 2H, Ar), 8.93 (s, 1H, N=CH). HRMS (EI) m/z calcd for $C_{17}H_{17}BrN_4O_2S$ 421.31, found 421.31.

4.12:- *N*-[3-(1-{(2*Z*)-2-[(5-bromopyridin-2-yl)methylidene]hydrazinyl}ethyl)-4,5,6,7-tetra hydro-1-benzothiophen-2-yl]acetamide (PI 40): Yield: 72.42%. mp: 166-168°C. IR (KBr) cm^{-1}: 3387, 3025, 2913, 1688, 694. ^{1}H NMR (DMSO-d6, 400 MHz) δ: 1.69-1.71 (m, 1H, CH2

{Ring}), 2.22 (s, 2H, CH_3), 2.61-2.83 (m, 1H, CH2 {Ring}), 8.95 (s, 1H, -CONH), 8.04-8.73 (m, 2H, Ar), 9.23 (s, 1H, N=CH). HRMS (EI) m/z calcd for $C_{17}H_{17}BrN_4O_2S$ 421.31, found 421.31.

4.13:- *N*-(3-{[(2*E*)-2-(2,4,5-trimethoxybenzylidene)hydrazinyl]carbonyl}-4,5,6,7-tetrahydro-1-benzothiophen-2-yl)acetamide (PI 44): Yield: 80.65%. mp: 165-167°C. IR (KBr) cm^{-1}: 3271, 3128, 2976, 1696. ^{1}H NMR (DMSO-d6, 400 MHz) δ: 1.68 (m, 1H, CH2 {Ring}), 2.20 (s, 2H, CH_3), 2.62-2.83 (m, 1H, CH2 {Ring}), 3.76 (s, 1H, -OCH3), 6.89 (s, 1H, -CONH), 6.50-6.89 (m, 2H, Ar), 9.94 (s, 1H, N=CH). HRMS (EI) m/z calcd for $C_{21}H_{25}N_3O_5S$ 431.51, found 431.51.

4.14:- *N*-(3-{[(2*E*)-2-(2-nitrobenzylidene)hydrazinyl]carbonyl}-4,5,6,7-tetrahydro-1-benzothiophen-2-yl)acetamide (PI 49): Yield: 65.65%. mp: 145-147°C. IR (KBr) cm^{-1}: 3367, 3059, 2942, 1522, 1334. ^{1}H NMR (DMSO-d6, 400 MHz) δ: 1.68-1.69 (m, 1H, CH2 {Ring}), 2.15 (s, 2H, CH_3), 2.61-2.83 (m, 1H, CH2 {Ring}), 7.21-7.66 (m, 2H, Ar), 9.86 (s, 1H, N=CH). HRMS (EI) m/z calcd for $C_{18}H_{18}N_4O_4S$ 386.43, found 386.43.

4.15:- *N*-(3-{[(2*E*)-2-(2-chloro-4-flurobenzylidene)hydrazinyl]carbonyl}-4,5,6,7-tetrahydro-1-benzothiophen-2-yl)acetamide (PI 51): Yield: 90.68%. mp: 157-159°C. IR (KBr) cm^{-1}: 3371, 3059, 2923, 1073, 777^{1}H NMR (DMSO-d6, 400 MHz) δ: 1.68 (m, 1H, CH2 {Ring}), 2.13 (s, 2H, CH_3), 2.61-2.83 (m, 1H, CH2 {Ring}), 6.75-7.38 (m, 2H, Ar), 9.78 (s, 1H, N=CH). HRMS (EI) m/z calcd for $C_{18}H_{17}ClN_3O_2S$ 393-86, found 393.86.

PHARMACOLOGICAL ASSESSMENT:

In Vitro Anticancer Screening (MTT Assay):

Principle: The MTT assay assesses cell viability and proliferation by utilizing MTT (3-(4,5-Dimethylthiazol-2-yl)-2,5-diphenyltetrazolium bromide), which is reduced to a purple formazan in living cells. The formazan is solubilized using solvents like DMSO, acidified ethanol, or SDS in HCl. Absorbance, measured at 500-600 nm, indicates cell viability, with higher absorbance reflecting a greater number of living cells.

Materials and Methods:

- **Cell Line and Culture:** MCF-7 cells (NCCS, Pune, India) were cultured in DMEM (Gibco, Invitrogen) supplemented with 10% FBS, L-glutamine, sodium bicarbonate, and antibiotics. Cells were maintained at 37°C in a 5% CO2 incubator.
- **Cell Seeding:** Cells were trypsinized, resuspended in 10% growth medium, and seeded at 5x10^4 cells/well in a 96-well plate. They were incubated for 24 hours at 37°C in 5% CO2.
- **Compound Preparation and Treatment:** Compounds were filtered through a 0.22 µm filter. After 24 hours, the medium was replaced with compound solutions (100 µg, 50 µg, 25 µg, 12.5 µg, 6.25 µg in 100 µl 5% DMEM) and incubated for an additional 24 hours.
- **MTT Assay:** MTT solution was prepared in FBS and filtered. Post-treatment, 3 µl of MTT was added to each well and incubated for 4 hours at 37°C. The formazan crystals were solubilized with 100 µl DMSO, and absorbance was measured at 540 nm using a microplate reader.

RESULTS AND DISCUSSION:

Key Compounds and Docking Analysis: The study centered on three principal compounds—PI 13, PI 40, and PI 5—from the PI series, which were selected for their promising enzyme selectivity based on molecular docking analyses. The docking studies revealed that these compounds exhibited strong alignment with the space-filling model of the 1M17 co-crystallized ligand, suggesting a high potential for effective binding. The docking simulations indicated that the presence of electron-withdrawing groups, especially hydroxyl groups on the aromatic ring, significantly enhanced binding affinity. The Glide module, utilizing flexible docking, hierarchical filters, and energy minimization with the OPLS-AA force field, provided comprehensive insights into ligand-receptor interactions. The top poses, selected based on G-Score, Glide Energy, and contact counts, are summarized in Table 2, which lists the 15 most favorable molecules from the PI series.

Table 2: Extra precision docking results for compounds belonging to PI Series

SN	Molecule ID	Docking score/ Glide Score	Glide energy
1	PI 13	-8.25	-52.728
2	PI 40	-7.085	-49.351
3	PI 5	-6.607	-43.241
4	PI 1	-6.276	-47.959
5	PI 8	-6.003	-47.007
6	PI 39	-5.889	-46.426
7	PI 6	-5.861	-47.277
8	PI 51	-5.849	-46.332
9	PI 44	-5.798	-45.895
10	PI 10	-5.769	-40.23
11	PI 28	-5.763	-43.91
12	PI 31	-5.706	-46.901
13	PI 49	-5.661	-44.429
14	PI 30	-5.659	-44.122
15	PI 36	-5.608	-45.808

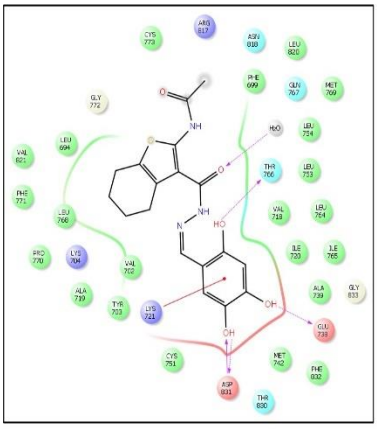

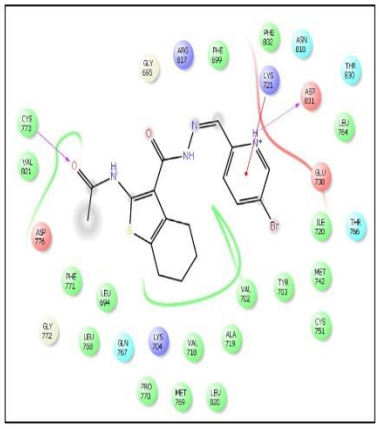

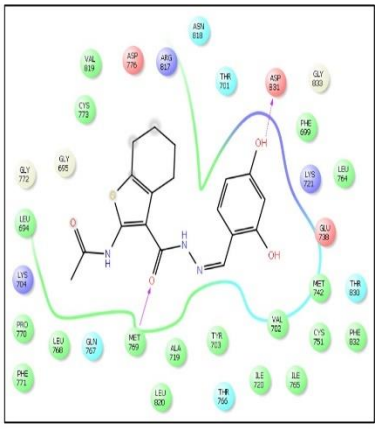

Figure 4: Binding of PI 13, PI 40 and PI 5 into the active site of 1M17 enzyme

Synthesis and Anticancer Activity: Based on favorable binding affinities, 15 compounds from the PI series were synthesized and their anticancer potential was evaluated. The in vitro assessment was conducted using the MTT assay on MCF-7 breast cancer cells, a colorimetric method that measures cell viability through the reduction of MTT to formazan by mitochondrial enzymes in living cells. This assay provided a quantitative measure of the cytotoxic effects of the synthesized compounds.

Anticancer Efficacy: Among the synthesized derivatives, PI 13 demonstrated the highest anticancer activity, with an IC50 value of 0.062 μM, indicating potent inhibition of MCF-7 cell proliferation. PI 40 and PI 5 also showed substantial anticancer activity, with IC50 values of 0.089 μM and 0.098 μM, respectively. The presence of electron-withdrawing groups, particularly hydroxyl groups on the aromatic ring, was correlated with enhanced anticancer activity. In contrast, compounds with nitro groups at the meta position or those containing five-membered rings like furan displayed lower efficacy, as indicated by higher IC50 values. (Table 3)

Correlation of Docking and Biological Activity: The results from the MTT assay were consistent with the predictions made in the molecular docking studies, demonstrating the reliability of the in silico methods employed. The strong correlation between docking scores and observed anticancer activity emphasizes the potential of these compounds as viable anticancer agents. The electron-withdrawing groups, which were identified in the docking studies as crucial for binding affinity, also played a significant role in enhancing the anticancer efficacy of compounds PI 13, PI 40, and PI 5. (Table 4 and Figure 5)

Table 3: IC50 Values and % Viability at Highest Concentration

Compound	IC_{50}	% Viability at Highest Concentration
PI 1	0.138	27.648
PI 5	0.098	27.422
PI 6	0.276	30.585
PI 8	0.185	28.219
PI 10	0.324	30.447
PI 13	0.062	22.791
PI 28	0.350	30.459
PI 30	1.205	33.271
PI 31	0.749	33.478
PI 36	1.328	34.369
PI 39	0.256	29.895
PI 40	0.089	24.881
PI 44	0.231	29.895
PI 49	0.599	32.888
PI 51	0.214	27.792

5-FU	0.021	18.654

Table 4: Comparative Data of Anticancer Activity and Glide Score

PI	Gscore	IC50
1	-6.276	0.138
5	-6.607	0.098
6	-5.861	0.276
8	-6.003	0.185
10	-5.769	0.324
13	-8.25	0.062
28	-5.763	0.35
30	-5.659	1.205
31	-5.706	0.749
36	-5.608	1.328
39	-5.889	0.256
40	-7.085	0.089
44	-5.798	0.231
49	-5.661	0.599
51	-5.849	0.214

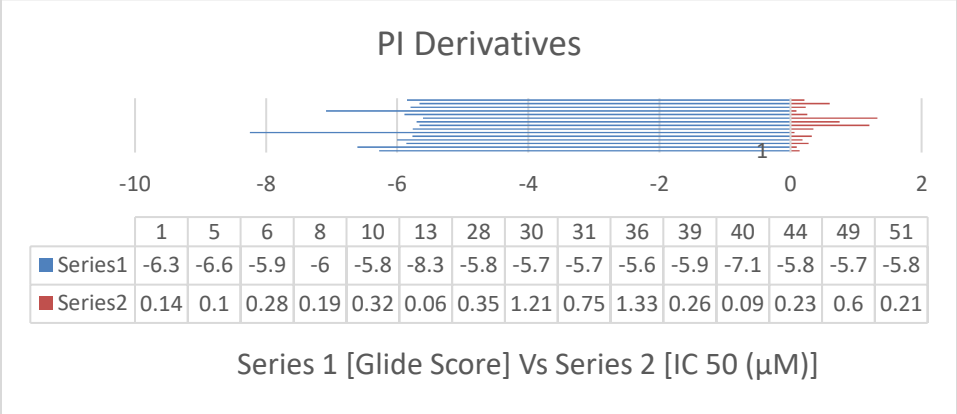

Figure 5: Graphical Presentation of Anticancer Activity and Glide Score

CONCLUSION:

This research effectively combined computational and synthetic approaches to identify and evaluate 4,5,6,7-tetrahydrobenzo[b]thiophene derivatives as potential EGFR inhibitors with notable anticancer activity. The alignment between docking predictions and in vitro results underscores the value of molecular modeling in drug discovery, providing a solid foundation for the development of targeted anticancer therapies. The compounds identified, particularly PI 13, show significant promise for further development and optimization as effective anticancer agents.

CONFLICT OF INTEREST:

None to declare

ACKNOWLEDGEMENTS:

The authors thank UGC, New Delhi, for funding the acquisition of the Schrodinger modeling suite under a Major Research Project, facilitated by the School of Pharmacy, Swami Ramanand Teerth Marathwada University, Nanded.

REFERENCES:

1. Kallioniemi OP, Kallioniemi A, Kurisu W, et al. ERBB2 amplification in breast cancer analyzed by fluorescence in situ hybridization. *Proc Natl Acad Sci.* 1992; 89: 5321–5325.
2. Hubbard SR, Till JH. Protein Tyrosine Kinase Structure and Function. *Annu Rev Biochem.* 2000; 69: 373-398.
3. Kolibaba KS, Druker BJ. *Biochim. Biophys. Acta.* 1997; 21: 1333.
4. Ross JS, et al. Targeted therapy in breast cancer: The HER-2/neu gene and protein. *Mol Cell Proteomics.* 2004; 3: 379–398.
5. Tzaha E, Waterman H, Chen X, et al. A hierarchical network of interreceptor interactions determines signal transduction by Neu differentiation factor/neuregulin and epidermal growth factor. *Mol Cell Biol.* 1996; 16: 5276–5287.
6. Moasser MM. The oncogene HER2: Its signaling and transforming functions and its role in human cancer pathogenesis. *Oncogene.* 2007; 26: 6469–6487.
7. Fleming TP, Saxena A, Ali IU, et al. Amplification and/or overexpression of platelet-derived growth factor receptors and epidermal growth factor receptor in human glial tumors. *Cancer Res.* 1992; 52: 4550.
8. Anido J, Matar P, Albanell J, et al. ZD1839, a specific epidermal growth factor receptor (EGFR) tyrosine kinase inhibitor, induces the formation of inactive EGFR/HER2 and EGFR/HER3 heterodimers and prevents heregulin signaling in HER2-overexpressing breast cancer cells. *Clin Cancer Res.* 2003; 9: 1274.
9. Wardakhan WW, Edrees M. Uses of 4, 5, 6, 7-tetrahydrobenzo[b]thiophene derivatives in heterocyclic synthesis: Synthesis of pyrazol, pyrimidine, and pyridazine derivatives with antimicrobial activities. *Egyptian Journal of Chemistry.* 2010; 53(2): 243-255.
10. Mohareb RM, Wardakhan WW, Abbas NS. Synthesis of Tetrahydrobenzo[b]thiophene-3-carbohydrazide derivatives as potential anti-cancer agents and Pim-1 kinase inhibitors. *Anti-Cancer Agents in Medicinal Chemistry.* 2019; 19(14): 1737-1753.
11. RCSB Protein Data Bank. Available from: www.rcsb.org.
12. Doyle M, Lente V, Mowat R, Fobare W. Alkyl nitrite-metal halide deamination reactions: Synthetic coupling of electrophilic bromination with substitutive deamination for selective synthesis of multiply brominated aromatic compounds from arylamines. *Bioorg Chem.* 1979; 28.
13. Sandmeyer TD. *Chem. Ges.* 1884; 17: 1633-1635.
14. Smith R, Angello B, Peterg B, et al. Reactions of Hydrazines with Esters and Carboxylic Acids. *Bioorg Chem.* 2010; 38: 2.